Proceedings of the
International Conference on Mechanical Engineering 2011
(ICME2011) 18-20 December 2011, Dhaka, Bangladesh

ICME11-AM-026

MICRO-MECHANICAL CHARACTERISTICS OF HUMAN BONE: A PRE-REQUISITE FOR CUSTOMIZED IMPLANT DESIGNING

Satarupa Biswas[1], **Promita Bhattacharjee**[1], **Krittika DasGupta**[1] **and Abhijit Chanda** [1, 2]

[1] School of Bioscience and Engineering, Jadavpur University,Kolkata, India.
[2]Mechanical Engineering Department, Jadavpur University,Kolkata, India.

ABSTRACT

Among the different types of implants used worldwide, hip implants are quite common. Not too many of them are customized or patient-specific. So far there have been number of studies on mechanical properties of bone but gender based variation in bone properties is not yet reported. The existing concept mostly revolves around the variation in overall size of male and female bone and it is generally assumed that the micromechanical aspects are more or less same. However the gender specificity of macro and micromechanical properties is of utmost importance as far as design of customized implants is concerned. The present work focuses on this important issue. Mechanical properties studied from load-deformation curves and indentation shown differences, composition and microstructure remaining same with respect to gender. Flexural rigidity was observed to be more uniform in males. Along the shaft of the femur, almost all the properties were found to vary from proximal to distal end.

Keywords: Area Moment of Inertia, Flexural Rigidity, Human Femur, Plasticity Parameter, Anisotropy, Osteon, Microstructure, Load-Deformation Curve.

1. INTRODUCTION

Since the time orthopedic implantation is in use, the prevailing practice was to put the standard sized replacement parts selected from a commercial range provided by manufacturers based on anthropometric data. There are always patients outside the standard range, between sizes, or with special requirements caused by disease or genetics. In that case the implant would fail much earlier. In fact, inspite of great care, total hip replacements fail due to instability and aseptic loosening. This is firstly because of weak interfacial bond between the implant and the surrounding living tissue, Wear induced osteolysis of the neighboring bone modulus being the second reason. Stress shielding effect due to mismatch of implant and bone is also equally responsible for implant failure. Thus proper selection of material as well as design of the implant can make an implant more durable or in other words successful. To solve this problem, people have started designing customized or patient specific hip implants [1-3]. To achieve this, among the different methods, rapid prototyping is considered to be the best suitable one [4, 5]. The term *rapid prototyping* (RP) refers to a class of technologies that can automatically construct physical models from Computer-Aided Design (CAD) data. Although several rapid prototyping techniques exist, the basic steps followed by the process are:

1. Creating a CAD model of the design
2. Converting the CAD model to stereolithography (STL) format
3. Slicing of the STL file into thin cross-sectional layers
4. Constructing the model layer by layer
5. Cleaning and finishing the model

In case of orthopedic implants, the formation of the design in CAD is guided by CT scan or MRI data taken from the patients. The stack of images obtained is used to reconstruct the structure of the required portion and hence dictate the construction of the implant. Not only standard implants, we can even think of replacing a fractured bone with the help this rapid prototyping technique.

Now, the CT scan images can give information regarding the structural and configurational property of the bone concerned [6]. The machine will be able to mimic the original structure of the femur head or the acetabulam before they are replaced from the body. But they are unable to provide any information regarding the mechanical strength of the bone. Thus the implant is not customized with respect to properties. But matching of porosity, hardness, elastic modulus is important to avoid failure due to stress shielding. Previous researches have shown that elastic modulus can be controlled by controlling the porosity of the material during its formation by RP technique [7]. But in order to decide on the porosity or modulus in turn, knowledge of the actual values becomes essential. Many people have confirmed to the fact that mechanical properties of cortical and trabecular bone are quite different. Again, anisotropy of cortical bone, its structural heterogeneity has widespread effect on the mechanical and configurational properties of the bone. All these aspects needs to be addressed during replacing a part of the bone.

In our study, we have thoroughly studied the mechanical as well as configurational properties of the femur in microscopic as well as macroscopic level which can contribute to a better designing of hip implants with greater durability.

2. METHODOLOGY

A total of seven femurs (4 from males and 3 from females) were collected from human cadavers. Some of them were pretreated and dried which had no specifications for preservation. Rest of them was fresh and preserved at -20^{o}C. After taking out from the refrigerator, the bones were cleaned with light detergent and a soft brush in order to remove the fats and muscle attachments. The whole bone was then cut into different segments. Cleaning of bone marrow was done with compressed air and then water jet. The pieces were preserved in formalin solution till the experiments were performed. For initial cutting, hand saw was used. But for accurate cutting which was required for different kinds of experimental procedures for studying micro behavior, low speed diamond saw was used. For those samples which required a polished surface, grinding and then polishing was done in the polishing machine (LECO Spectrum System 1000, USA) using cloths of different grit size. The surface roughness of these polished surfaces was measured by Tallysurf Profilometer. For each case, Centerline Average value <0.25 micron was ensured.

For observing the macro-mechanical properties, samples of different sizes were cut and prepared following the ASTM standard (ASTM F 451 RE). The samples were uniaxially loaded under compression, i.e. the sample was placed between two flat discs and a load of 5KN was allowed at the head at a constant rate or cross head speed of 0.5mm/minute. This rate was also varied till 3mm/min to observe the effect of rate of loading. From this loading in Universal Testing Machine (UTM: INSTRON 4204, U.K.), a constant load-deformation curve was obtained for both tension and compression from which, a number of information regarding the behavior of the material during loading. Young's modulus and work of fracture was calculated from the load-deformation curve itself.

The macro-hardness test of the polished samples was done using Vicker's Hardness testing machine (LV 700AT, LECO, USA). The loads applied during the indentation were 0.5kgf, 1kgf and 3kgf. Number of indentations was made for each load on each sample. Both transverse and longitudinal directions were considered and a distance of at least thrice the impression diagonals were maintained between two consecutive indents to avoid interactions between indentations. Lamella and interstitial regions were separately indented at each load. The diagonals of the impression were measured immediately after indentation to obtain the hardness values. Two other sets of readings were taken from the same impressions after 15 minutes and 30 minutes respectively to observe any possible viscoelastic contraction of the impression.

The indented samples were put into critical point drier to remove the presence of any liquid inside the pores and then gold coated to observe under Scanning Electron Microscope (SEM). The images of the cracks formed due to indentation were taken in the secondary electron mode.

Depth sensitive indentation (DSI) popularly termed as nanoindentation technique, was done as described by Oliver and Pharr [8]. The present tests were conducted on a Fisheroscope (H100, Fischer, Germany) following standard protocol and values for the required parameters were obtained. In our experiment, a 3x3 matrix was chosen within a confined rectangular area avoiding visible pores as much as possible. The maximum and residual depths were noted from where plasticity parameter (h_f /h_{max}) could be calculated. Also all the loading-unloading curves were studied individually for any kinks, pop-in or pop-out which can indicate onset of crack formation.

Flexural rigidity is a term obtained from the product of elastic modulus of the material and area moment of inertia. When this flexural rigidity is high, the resistance to bending moment is also high and since it is proportional to the area moment of inertia, observing the trend of this moment might provide us information regarding this configurational property of the bone. Computed Tomography (CT) images of the lower extremities were collected from CMRI Hospital, Kolkata. In a CT Machine X-ray slice data is generated using an X-ray source that rotates around the object. For each patient, numbers of slices of the image was obtained from the software and finally we had around 30 cross sectional images of both the femurs. Image processing was done with the help of MATLAB v 6.0. With a simple code, the cross sectional area of the region of interest and the centroid could be found out. The area moment of inertia was calculated from the processed image slices using IMAGE J image analysis software.

3. RESULTS AND DISCUSSION

After thoroughly studying the load deformation curves for both male and female samples it was observed that the initial part showed a stunning similarity for all the samples both in male and female. The load deformation curve could be differentiated into two zones i.e., the elastic zone which was linear in all cases, and a nonlinear post yield zone. Under compression, after reaching the peak load the curve was more flat in females than in males. The nonlinear zone was basically the fracture zone where each sample behaved differently but followed a definite trend. Figure-1 shows a representative curve for the load deformation curves in both male and female with error bars showing 5-10% scatter. The ultimate stress and work of fracture for both male and female samples are shown in table 1. The difference in the average values of work of fracture has been around 10% which is well within possible experimental scatter. Rather we should say the values were quite comparable. This strongly contradicts the prevailing hypothesis of higher vulnerability of female bone due to increased porosity particularly at higher age.

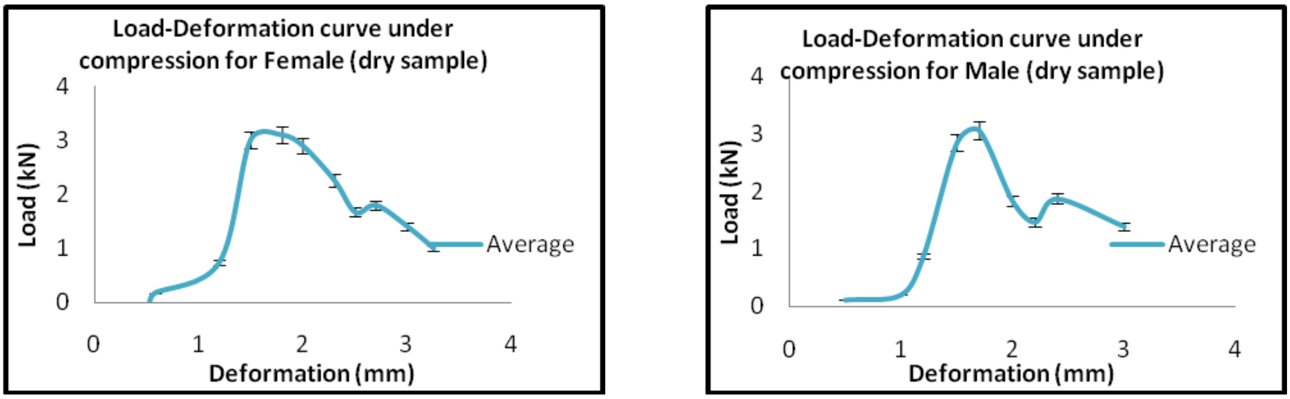

Fig 1. Representative Load-deformation curves for dry, pretreated bones in male and female samples

Table 1: measurements from load-deformation curves

	Male	Female
Ultimate Compressive Stress(MPa)	*198.5*	*196.27*
Work of fracture(N-mm)	*3888.65*	*3974.5*

Rate of loading also plays an important factor while observing the behavior of the bone. Figure 2a shows the change in stiffness with increasing cross head speed.

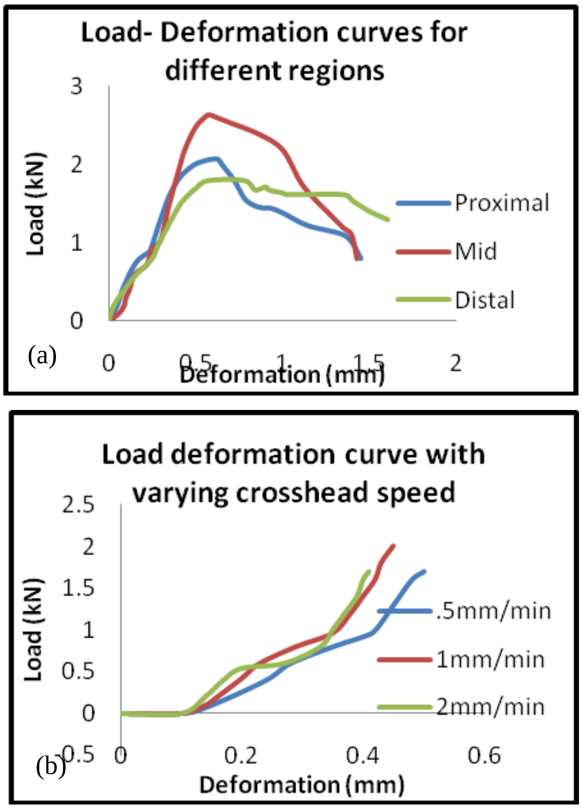

Fig 2. Load-deformation curves (a)with varying cross-head speeds in male and female samples, (b) along different regions of the shaft

This indicates that while designing an implant, not only age, but the regular activity of the person along with his professional requirements should also come under consideration. Higher the loading rate of the bone, higher will be the stiffness of the bone. Another parameter for variation was considered within the same study. This is the region of interest along the femur shaft. Samples from the cortical part of proximal, mid and distal shaft were considered. The curves in figure 2b showed that the middle part is the steepest, could sustain more load and hence has got the maximum work of fracture.

Cortical bone shows a standard hierarchical structure which is responsible for the heterogeneity of the properties in bone. It shows variable directional properties. Anisotropy of bone was already previously established in the macroscopic level. In this study we have also considered the local level heterogeneity induced differences in mechanical properties through the indentation technique.

The hardness was measured in different directions along the axis of the bone. The cross section, i.e., along the longitudinal direction showed consistently lower hardness values as compared to the transverse direction. In the cross sectional surface, distinguished lamellar and interstitial zones showed varied hardness values. The interstitial zone consistently showed higher hardness values than the lamellar region. This may be attributed to the higher mineralization of the extracellular matrix and also orientation of the collagen fibers along the osteons and in the interstitial region. Table 2 shows how the hardness differ in lamellar and interstitial region.

Hardness was also tested along different parts of the shaft. The whole shaft was divided into three major parts – Proximal part, mid diaphysis and the distal part. It was observed that in both pretreated and fresh bones the Vicker's hardness values gradually increased from proximal to distal part. Generally for most of the materials when hardness increases, we can say that the toughness decreases. In general we know that distal fracture is more common in femurs. This is also in accordance with our finding as in our study, the hardness steadily increased from proximal to distal end. Therefore it is expected that toughness will decrease and thus the distal end becomes more prone to fracture.

Table 2: Hardness values in Hvperformed in different directions.

	Fresh				Pretreated			
	Male		Female		Male		Female	
Load(kgf)	0.5	1.0	0.5	1.0	0.5	1.0	0.5	1.0
Longitud-inal	33.25	38.89	32.94	40.48	36.6	36.3	27	28.66
Transverse	28.63	35.53	28.5	30.06	38.06	37.33	20.4	30.13

Perhaps this may be attributed to the higher osteonal density at the distal part rather than the proximal part. However, this has to be validated with a much detailed study.

Nano-indentation of sections of the cortical part gave hardness values in GPa. For both male and female, the values were close to the micro-indentation values. But as load decreased, hardness increased, clearly indicating the presence of indentation size effect. In general, indentation size effect is visible in crystalline structures. The nano-crystals of mineral apatite present as an integral part of its structure may be responsible for this kind of effect. While performing this DSI experiment, a program was selected with 3x3 matrix that made as many as 25 indents and subsequently same number of load-deformation curves were obtained. Out of them, around 30% showed erratic behavior at the lowest load i.e. 10mN. Few of the indents might have fallen on haversian canals or over some subsurface pores and cause such scatter. We discarded the erratic curves and considered the curves of similar pattern forming a band. However, as the load was increased, this percentage of erratic behavior decreased. Still we considered only the uniform curves so as to obtain the load-dependent response from structurally homogeneous region. A definite trend was observed. Hardness was as high as 0.88GPa±0.02 at the minimum load of 10mN. Then there was a drastic drop till 0.4 GPa after which the decrease was less in proportion with increasing load.

The curves obtained from nano-indentation in all the loads were studied in details for any major features of pop-in or pop–out. Each curve was divided into zones and enlarged (as shown in the inset image of figure 3) but no such characteristics were observed. This also indicates that there is no sudden onset of plasticity and thus it is very difficult to predict any crack initiation during the process of indentation.

The young's modulus could also be obtained from this type of indentation method. The elastic modulus obtained from nano-indentation technique varied from 10.59GPa to 13.02 GPa. But the elastic modulus that we have obtained from other techniques like compressive loading in Universal testing machine gave values much less than this. This may be due the fact that results from UTM gave an aggregate or averaged value whereas in case of nano-indentation, the result gave the modulus of very specific regions. Thus it is important to understand how the elastic modulus is varying in different regions of the femur shaft.

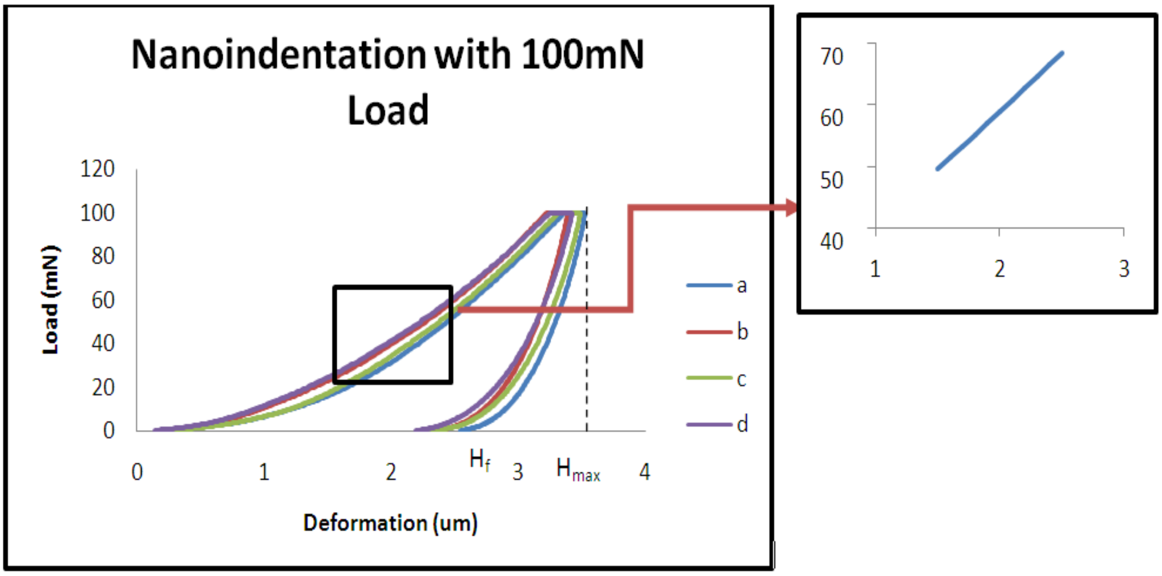

Fig 3. Load-deformation curve during loading and unloading obtained from nanoindentation.

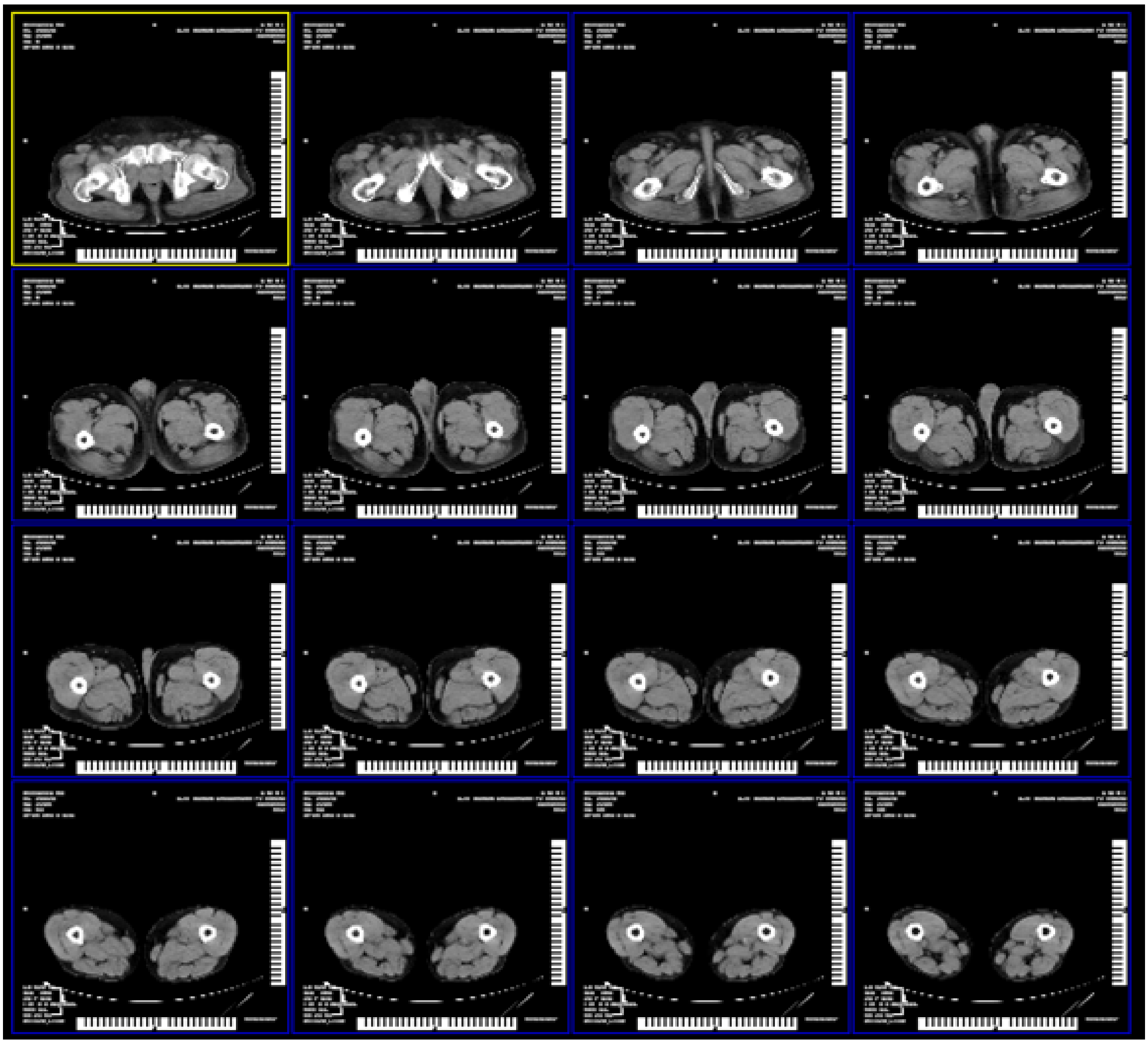

Fig 4. Typical CT scan data for pair of femurs for a female patient wherefrom area and area moment of inertia were calculated using Standard Image analysis software

The femur bone has a columnar structure and it experiences maximum compressive load. Thus there are chances that the bone may bend or buckle. But nature has created its geometry in such a way that it is optimized and does not bend normally. Resistance to this bending is given by the flexual rigidity for which knowledge of the area moment of inertia is required. CT Scan images were used here to determine the cross sectional area and the moment of inertia. The cross sectional area of the cortical region of the entire shaft of both right and left femur was calculated in MATLAB for four specimens, two from male patients and two from female. The age groups considered were middle aged to old age. The head and the distal part of the femur was not considered because of their spongy nature. Critical analysis showed a particular trend of variation of the cortical area along the shaft of the femur. This trend (Figure 4) shows there can be an increase at the distal part as well.

Although there is not much variation in the trend when compared to male and female patients, area moment of inertia showed different results. Since femur is mostly subjected to loading of this type, resistance to bending must be a phenomenon of importance. As the structure itself is an optimized one, we attempted to find out any specific trend that it follows which can guide the specific design considerations of the implant. By taking the figures as equivalent ellipse, approximate values of area and area moment of inertia were calculated and the graphs obtained are shown in figure 5 and 6.

Though the trend in the cross-sectional area in male and female are quite similar, the pattern of variation of the moment of inertia is different. Primarily, the slopes were different. In both the cases the overall resistance pattern to bending changes. In females, the fluctuation at the initial part is quite high (absolute value varies from15000 to 90000), whereas in males the fluctuation is less and the absolute values varied only between 30000 to 50000. Now, less of fluctuation apparently means more uniform resistance to bending in male, however we need higher sample size for generalization.

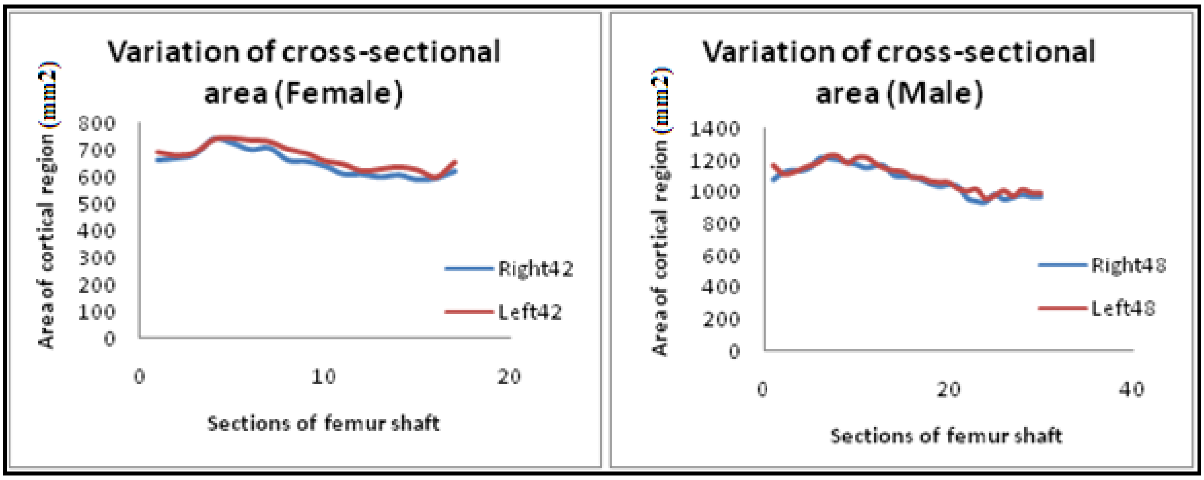

Fig 5. Variation of cross-sectional area of cortical part in (a) female and (b) male

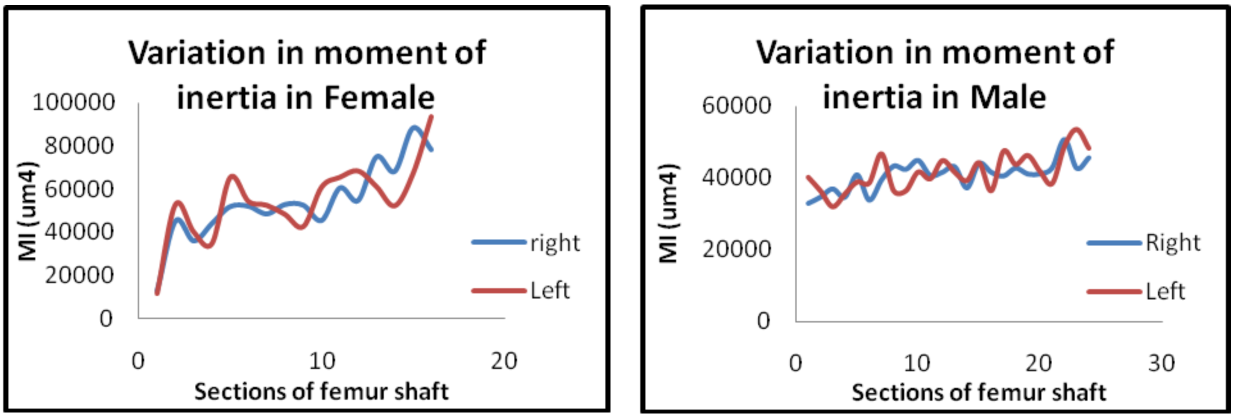

Fig 6. Variation in area moment of inertia of right and left femur shaft of(a) female and (b) male patients

4. CONCLUSION

From the study it is clearly observed that femur bone with a hierarchial structure shows anisotropy in its structure as well as its mechanical behavior. If we consider hip replacement of different genders, it is not merely a fact that size is the only thing that matters. In fact we must ensure the variation in mechanical behavior while constructing the artificial femur or a part of it. Generally the hip implants are cast, machined and finally push-fit into the bone cavity. While doing this exercise, the gender based variation in area moment of inertia along the length of the femur is also to be taken care of. Micro-mechanical properties like micro and nano hardness, stiffness, plasticity parameters reported in this work are also to be used for customized hip or femur design. We need a complete mapping of not only bone structure but also functional behaviours of bone for such design. The present work is an initiation in this direction.

6. REFERENCES

1. Götze C, Vieth V, Meier N, Böttner F, Steinbeck J, Hackenberg L., 2005, “CT-based accuracy of implanting custom-made endoprostheses.” Clinical Biomechanics, 30: 856-86
2. Ramos A, Completo A., Relvas C., Simões J.A., 2011, “Design process of a novel cemented hip femoral stem concept. Materials & Design” 33: 313-32
3. Sridhar I, Adie P.P., Ghista D.N., 2010, “Optimal design of customized hip prosthesis using fiber reinforced polymer composites.” Materials & Design, 30:6: 2767-2775
4. España F.A., Balla V.K., Bose S., BandyopadhyayA., 2010. “Design and fabrication of CoCrMo alloy based novel structures for load bearing implants using laser engineered net shaping.” Materials Science and Engineering C 30: 50–57
5. Rapid Prototyping Primer by William Palm (May 1998), revised 30 July 2002, Penn State Learning Factory.
6. Kawate K, Ohneda Y, Ohmura T, Yajima H, Sugimoto K, Takakura Y., 2009, “Computed Tomography–Based Custom-Made Stem for Dysplastic Hips in Japanese Patients.” The Journal of Arthroplasty24:1:65-70
7. Bandyopadhyay A., Espana F., Balla V.K., Bose S., Ohgami Y., Davies N.M., 2010, “Influence of porosity on mechanical properties and in vivo

response of Ti6Al4V implants.” Acta Biomaterialia 6: 1640–1648
8. Oliver, W. C., and Pharr, G. M., 1992 “An improved technique for determining hardness and elastic modulus using load and displacement sensing indentation experiments”, J. Mater. Res.,7: 1564.

7. MAILING ADDRESS

Satarupa Biswas
School of Bioscience and Engineering,
Jadavpur University,Kolkata-700032, India.